Photon sorters and QND detectors using single photon emitters

D. Witthaut,[1,2] M. D. Lukin,[3] and A. S. Sørensen[1]

[1] *QUANTOP, Niels Bohr Institute, University of Copenhagen, DK–2100 Copenhagen Ø, Denmark*
[2] *Max-Planck-Institute for Dynamics and Self-Organization (MPIDS), D–37077 Göttingen, Germany*
[3] *Department of Physics, Harvard University, Cambridge MA 02138*

(Dated: March 16, 2012)

We discuss a new method for realizing number-resolving and non-demolition photo detectors by strong coupling of light to individual single photon emitters, which act as strong optical non-linearities. As a specific application we show how these elements can be integrated into an error-proof Bell state analyzer, whose efficiency exceeds the best possible performance with linear optics even for a modest atom-field coupling. The methods are error-proof in the sense that every detection event unambiguously projects the photon state onto a Fock or Bell state and imperfections only result in reduced success probability, not in wrong results.

PACS numbers: 03.67.-a, 42.50.Ex, 42.50.Pq

I. INTRODUCTION

Experimental realization of number-resolving, non-demolition photo (QND) detectors is a long-standing challenge in quantum optics and quantum information science. Progress has been made in the microwave regime [1–4], but the optical regime remains an unsolved challenge. Conventional photodetectors measure only the intensity or the energy of an incoming light pulse, and are not capable of measuring photon states in a QND fashion. More advanced measurements schemes can be constructed using optical non-linearities, but these are typically very weak since photons rarely interact with each other. In this Letter, we show how to overcome this problem by exploiting strong coupling of light to individual single photon emitters. This provides a strong optical non-linearity (cf.[5]), which enables the realization of number-resolving photon sorters and quantum non-demolition photo detectors.

A common approach to realizing strong coupling between photons and emitters relies on cavity quantum electrodynamics (QED), where the light field is confined to a high–Q optical resonator [6, 7] or a microcavity [8–10]. An alternative approach is to use single emitters coupled to one dimensional photonic waveguides and great advances have been made using tapered optical fibers coupled to a single atom [11], microwave transmission lines coupled to a flux qubit [12], or surface plasmons modes coupled to a single photon emitter [5, 13–15]. In these systems the emitter couples to a continuous one-dimensional spectrum of modes and photon scattering is governed by the interference of absorbed, reemitted, and directly transmitted waves [16–19]. In a similar way, the transmission of a tighly focussed light beam can be controlled by a single emitter in free space [20, 21]. In the present paper we will explore possible applications of emitters coupled to such a one-dimensional photonic continuum for photo detection, but the ideas and formalism we use can also be applied to cavity QED as well as other methods of achieving strong optical non-linearities [10, 22–24].

First, we consider passive devices based on simple two-level emitters. The interaction with the emitter naturally leads to a photon sorter effect, which can be used to implement a number resolving photo detector. Secondly, we consider a waveguide coupled to a three-level emitter controlled by a classical laser field. This setup offers significantly more opportunities at the expense of a more complex setup. In particular we discuss QND photo detectors. As a possible application of these devices we will show how to construct optical Bell-state analyzers. A Bell measurement is an essential ingredient in quantum information, as it enables efficient quantum repeaters [25] as well as universal optical quantum computers [26]. Unfortunately such a measurement cannot be realized with linear optics [27], but requires a strong nonlinearity. We focus on realistic systems with losses and discuss how to make devices error-proof. Even in the case of an error, a measurement shall at most give an inconclusive but never a wrong result. This is important for many devices in quantum communication, in particular quantum repeaters [25], where incorrect measurement outcomes spoil the results whereas inconclusive outcomes only increase the necessary resources.

II. WAVEGUIDE QUANTUM OPTICS

To begin with, we briefly review the theory of photon scattering in a (semi-) infinite single-mode waveguide introduced in Refs. [16–19]. Following this approach, the photon field is decomposed into a left- and a right-moving mode described by the bosonic field operators $\hat{a}_L(x)$ and $\hat{a}_R(x)$, respectively. We assume that the photons have a linear dispersion relation with propagation velocity c for the entire frequency range of interest. The light-field couples to a single emitter placed inside the waveguide or in the evanescent field.

For some systems the most efficient coupling is realized by placing the emitter at one end of a semi-inifinite waveguide instead of side-to-side, in particular for plasmonic waveguides [5]. For these systems we take the po-

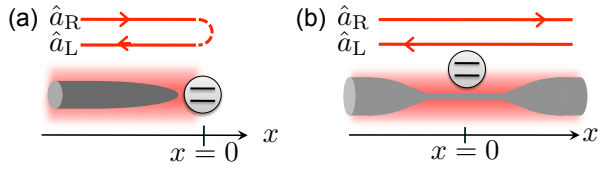

FIG. 1: Sketch of potential experimental setups illustrating the used coordinate system and the naming of the optical modes. (a) End-coupling as proposed for plasmonic waveguides [5]. (b) Side-coupling to a tapered optical fibers [11].

sition of the end of the guide to be $x = 0$. The propagation of the right- and left-going modes is then restricted to $x < 0$, cf. Fig. 1 (a). In this case we introduce the mode function

$$\hat{a}_e(x) = \begin{cases} \hat{a}_R(x) & \text{for } x < 0 \\ \hat{a}_L(-x) & \text{for } x > 0, \end{cases} \tag{1}$$

such that $x < 0$ describes the incoming and $x > 0$ the reflected photons. The free photon field is then described by the Hamiltonian

$$\hat{H}_{\text{free}} = -\mathrm{i}c \int \mathrm{d}x\, \hat{a}_e^\dagger(x) \frac{\partial}{\partial x} \hat{a}_e(x). \tag{2}$$

The coupling to the emitter is assumed to be local at the position of the end, $x = 0$. Within the rotating wave approximation, photon scattering is then described by the Hamiltonian

$$\hat{H} = \hat{H}_{\text{atom}} + \hat{H}_{\text{free}} + \sqrt{\Gamma} \int \mathrm{d}x\, \delta(x) \left(\hat{S}_- \hat{a}_e^\dagger(x) + \hat{S}_+ \hat{a}_e(x) \right), \tag{3}$$

where $\hat{S}_+ = \hat{S}_-^\dagger$ is an atomic raising operator. We set $\hbar = 1$, thus measuring all energies in frequency units. The coupling strength is here parametrized by the rate of spontaneous emission into the waveguide Γ.

If the emitter is coupled to a waveguide extending in both directions, we have to keep both the left- and the right-moving modes $\hat{a}_L(x)$ and $\hat{a}_R(x)$, cf. Fig. 1 (b). Nevertheless, the emitter only couples to the symmetric mode $\hat{a}_e(x) = (\hat{a}_R(x) + \hat{a}_L(-x))/\sqrt{2}$, again taking the position of the emitter as zero. Thus we recover the Hamiltonian (3) also in this setup. Below we focus on the semi-infinite case, which is conceptually simpler. However, the same detectors can be realized for waveguides extending in both directions by directing any incident photon to a balanced beam splitter to prepare a symmetric superposition of left and right moving modes.

The basic scattering problem for one photon interacting with a two-level emitter has been solved in [16]. In this case we have $\hat{H}_{\text{atom}} = (\omega_0 - i\gamma/2)|e\rangle\langle e|$ and $\hat{S}_+ = |e\rangle\langle g|$, where $|g\rangle$ and $|e\rangle$ are the ground and excited state of the emitter, respectively. Similar to the quantum jump approach [28] we have added an imaginary part to the resonance frequency of the emitter $\omega_0 - i\gamma/2$ describing a coupling of the emitter to other modes than the waveguide with a rate γ. Using the Lippmann Schwinger formalism one can then show that a monochromatic input state with wave number k is scattered as

$$|\Psi_{\text{in}}\rangle = \hat{a}_k^\dagger|0\rangle \quad \longrightarrow \quad |\Psi_{\text{out}}\rangle = t_k \hat{a}_k^\dagger|0\rangle. \tag{4}$$

Here, $|0\rangle$ denotes the vacuum state, i.e. the empty waveguide, and the operator $\hat{a}_k^\dagger$, defined as the Fourier transform of $\hat{a}_e^\dagger(x)$, creates a photon with wave number k. The transmission amplitude is given by [16]

$$t_k = \frac{ck - \omega_0 + \mathrm{i}(\gamma - \Gamma)/2}{ck - \omega_0 + \mathrm{i}(\gamma + \Gamma)/2}. \tag{5}$$

If losses are negligible, $\gamma = 0$, the photon thus experiences only a phase shift which equals π on resonance $ck = \omega_0$. If the emitter is side-coupled to an infinitely extended waveguide, an incident photon is reflected with a probability $|1 - t_k|^2/4$, which can be shown by transforming back to left- and right-moving modes. Scattering by a three-level emitter was discussed in detail in ref. [19].

When two or more photons enter the waveguide simultaneously, scattering by a two-level emitter induces an effective photon-photon interaction, which is extremely useful for the detection and manipulation of light fields. Here we consider an input state of two identical photons with pulse shape $f_{2,\text{in}}(k,p) = f_1(k)f_1(p)$,

$$|\Psi_{\text{in}}\rangle = \frac{1}{\sqrt{2}} \int \mathrm{d}k\, \mathrm{d}p\, f_{2,\text{in}}(k,p)\, \hat{a}_k^\dagger \hat{a}_p^\dagger |0\rangle, \tag{6}$$

where k and p denote the wave numbers of the two photons. The interaction with a single two-level emitter introduces strong correlations of the two photons

$$f_{2,\text{out}}(k,p) = t_k t_p f_1(k) f_1(p) + f_B(k,p). \tag{7}$$

Here, the subscript B refers to a 'bound state' contribution, whose precise form can be found in Refs. [17, 18].

Let us briefly comment on the applicability of the theoretical model and possible errors in an experimental realization. The most obvious source of errors is the imperfect coupling of the emitter to the waveguide. This is taken into account by the coupling rate γ to other modes than the waveguide. Indeed, the success probability of all devices introduced in this letter crucially depends on the ratio Γ/γ. Currently, the most advanced experimental setup employs a microwave transmission line side-coupled to a flux qubit. In this experiment, a photon incident from the side was back-scattered with 94% probability. Translated into the current setting this corresponds to a coupling of $\Gamma/\gamma \approx 32$. In the optical regime, a strongly increased decay rate was demonstrated for single quantum emitters coupled to a surface plasmon polariton mode on a silver nanowire [14]. For a single diamond color center, an increase by a factor of 3.6 was reported [15]. This suggests (but does not prove) $\Gamma/\gamma \approx 2.6$. The second major source of errors is photon absorption in the waveguide. While this process is negligible for tapered optical fibers

and free space setups [10, 11, 20, 21], losses are particularly strong in plasmonic systems. In such an experiment a rapid in- an outcoupling to a dielectric waveguide is inevitable (cf. [5]). However, we note that absorption is a general problem which is equally present in linear photo detectors. In addition, all measurement schemes presented in this letter are designed such that photon loss may lead to inconclusive, but not to incorrect results. In particular, a successful Bell state measurement always requires the coincidence detection of both incident photons for the setup presented below as well as for any setup based on linear optics. Hence inefficient detectors would suppress both linear optics and the more advanced detectors presented here by the same amount. Additional coupling losses can easily be accounted for by multiplying our resulting success probabilities by the probability for the photons not to be lost. A less obvious, but more critical issue is the dispersion of properties from emitter to emitter, especially in a solid-state realization. This source of errors is analyzed in detail below for the photon sorter device.

III. PHOTON SORTER

One of the conceptually simplest extensions of linear optics is a device capable of non-destructively distinguishing single and two photon pulses. Such a photon sorter can be realized with only passive optical elements and simple two level emitters using the setup sketched in fig. 2.

We assume that the incoming pulse enters the interferometer in the upper arm labelled by $\hat{a}_{\rm in}$. A single photon wave packet is split at the beam splitter and brought to interact with the emitters, where it experiences the phase shift (5). This phase depends on the wavenumber k but is the same in both arms of the interferometer. The interferometer can therefore be balanced such that a single photon always leaves the setup in mode $\hat{a}_{\rm out}$. This is different if two photons enter the setup and interact indirectly via the emitter in which case they can leave the interferometer in mode $\hat{b}_{\rm out}$ with a significant probability. To be more precise, we consider an input state of two identical photons (6) with pulse shape $f_2(k,p) = f_1(k)f_1(p)$. The beam splitter mixes the modes $\hat{a}$ and $\hat{b}$ such that $\hat{a}_k^\dagger\hat{a}_p^\dagger \to \hat{a}_k^\dagger\hat{a}_p^\dagger + 2\hat{a}_k^\dagger\hat{b}_p^\dagger + \hat{b}_k^\dagger\hat{b}_p^\dagger$. When both photons are in the same mode, the interaction with the emitter introduces the strongly correlated 'bound state' contribution (7). Finally, after interacting with the beam splitter once again, the two-photon input state is transformed to

$$|\Psi_{\rm out}\rangle = \frac{1}{2\sqrt{2}}\int {\rm d}k{\rm d}p\, f_B(k,p)\hat{b}_k^\dagger\hat{b}_p^\dagger|0\rangle \qquad (8)$$
$$+\frac{1}{\sqrt{2}}\int {\rm d}k{\rm d}p\left(t_k t_p f_1(k)f_1(p) + \frac{1}{2}f_B(k,p)\right)\hat{a}_k^\dagger\hat{a}_p^\dagger|0\rangle.$$

Note that there are no mixed terms (e.g. $\hat{a}_k^\dagger\hat{b}_p^\dagger$), so that the two photons always leave the interferometer in the same arm. There is a significant probability that the two photons leave the setup in mode $\hat{b}_{\rm out}$, whereas a single photon always leaves the interferometer in mode $\hat{a}_{\rm out}$, such that the interferometer acts as a photon sorter.

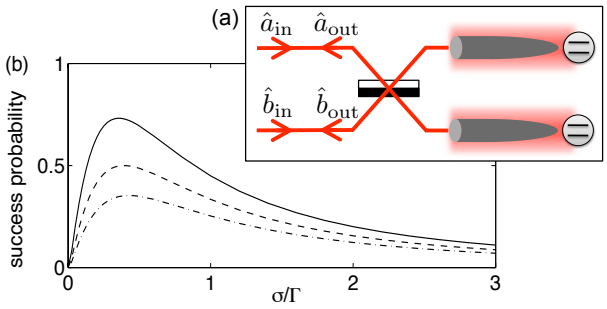

FIG. 2: (a) A photon sorter based on a 1D waveguide end-coupled to a single emitter. A single photon will always leave the photon sorter in mode $\hat{a}_{\rm out}$, while two photons are likely to leave in mode $\hat{b}_{\rm out}$ but never split into one photon in each arm. (b) The success probability of the photon sorter, i.e. the probability that two photons are scattered to the mode $\hat{b}_{\rm out}$, as a function of the frequency width σ of a Gaussian input pulse for $\gamma/\Gamma = 0$ (solid line), $\gamma/\Gamma = 0.1$ (dashed line), and $\gamma/\Gamma = 0.2$ (dash-doted line), respectively.

The success probability of the photon sorter, i.e. the probability that two photons are scattered to the mode $\hat{b}_{\rm out}$ is given by

$$p_s = \frac{1}{4}\int {\rm d}k{\rm d}p\,|f_B(k,p)|^2. \qquad (9)$$

The success probability is shown in fig. 2 (b) for a Gaussian input pulse $f_1(k) \sim \exp(-(ck-\hbar\omega_0)^2/4\sigma^2)$ as a function of the frequency width σ. One observes that the efficiency of the photon sorter strongly depends on the pulse shape of the incident photons. They must be resonant to the atomic transition and the frequency width σ should therefore not be too large. On the other hand the photons should be tightly localized in real space as they only interact when they are at the same position. Thus an optimum value of the efficiency is found for intermediate values of σ.

Regardless of the success probability the photon sorter can provide insight into the nature of the incoming light pulse. If for instance a conventional photo detector detects the output in mode $\hat{b}_{\rm out}$, the intensity of that measurement directly reflects the two photon contribution in the pulse. In addition, the success probability can be increased in an array of concatenated devices by feeding the output mode $\hat{a}_{\rm out}$ of one sorter to the next one. For example, an array of five photon sorter increases the success probability to 96 % for $\sigma/\Gamma = 0.36$ and $\gamma = 0$.

Coupling losses or photon absorption may reduce the success probability, but will not cause an incorrect routing of a single photon. However, such a more crucial error can occur if the properties of the emitters in the two interferometer arms are significantly different. The

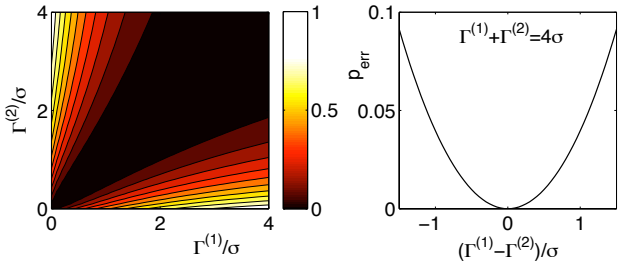

FIG. 3: Error probability (10) of a photon sorter due to a variation of the coupling rate $\Gamma^{(1,2)}$ in the two arms of the interferometer for a Gaussian input pulse with frequency width σ.

probability that a single photon is spuriously transmitted to the mode $\hat{b}_{\rm out}$ is then given by

$$p_{\rm err} = \frac{1}{4}\int dk\, |f_1(k)(t_k^{(1)} - t_k^{(2)})|^2, \qquad (10)$$

where the superscripts (1), (2) label the transmission amplitude (5) for the two arms or the interferometer. This probability is plotted in fig. 3 for the case of two different coupling rates $\Gamma^{(1,2)}$ and $\gamma = 0$. The error probability $p_{\rm err}$ vanishes quadratically with the difference $\Gamma^{(1)} - \Gamma^{(2)}$, such that small variations in the coupling rates have only weak effects.

IV. QUANTUM NON-DEMOLITION DETECTOR

To realize more advanced photo detection schemes we shall now consider three-level emitters as also discussed in Refs. [5, 7, 29]. Generalizing these approaches, we now describe how to construct a QND photo detector using the setup shown in fig. 4 (a). A three-level emitter is prepared in a coherent superposition of the ground state $|g\rangle$ and a metastable state $|s\rangle$, which does not couple to the waveguide,

$$|g\rangle \longrightarrow \alpha|g\rangle + \beta|s\rangle, \quad \text{and} \quad |s\rangle \longrightarrow -\beta|g\rangle + \alpha|s\rangle, \quad (11)$$

with $\beta = \sqrt{1-\alpha^2}$. A passing resonant photon then introduces a phase shift if and only if the emitter is in state $|g\rangle$. In particular the transmission amplitude (5) on resonance is given by $t_0 = (\gamma - \Gamma)/(\gamma + \Gamma)$. Then one applies another classical control pulse which inverts the transformation (11). The complete procedure thus realizes the mapping

$$\begin{aligned} &1 \text{ photon:} \quad |g\rangle \to (\beta^2 + t_k\alpha^2)|g\rangle + \alpha\beta(1-t_k)|s\rangle, \\ &0 \text{ photons:} \quad |g\rangle \to |g\rangle. \end{aligned} \qquad (12)$$

If the state of the emitter is now measured to be $|s\rangle$, e.g. by measuring the phase shift imprinted on an incident classical laser beam afterwards, this unambiguously reveals the presence of a single photon. Unlike conventional

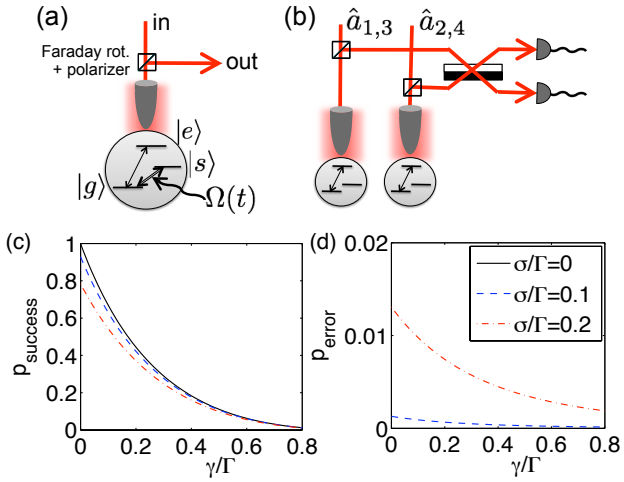

FIG. 4: (a) A QND photo detector based on a three-level emitter strongly coupled to a one-dimensional waveguide. A Faraday rotator combined with a polarizer separates the incident and the reflected mode into two spatially separated modes. (b) Integration of the QND photo detector in a Bell state analyzer. The control photon (modes $\hat{a}_{1,2}$) passes the setup before the target photon (modes $\hat{a}_{3,4}$). (c,d) The success and error probabilities as a function of the scaled decay rate γ/Γ for a Gaussian input pulse for different values of the width σ.

photo detection this does not disturb the photon, i.e. the scheme realizes a QND measurement. Furthermore if no photon is present, the emitter returns deterministically to the initial state $|g\rangle$, i.e. there are no dark counts. The optimal detector efficiency is reached for $\alpha = 1/\sqrt{2}$ and is given by $\Gamma/(\gamma+\Gamma)$, which approaches unity when $\Gamma \gg \gamma$. Using the microwave system of ref. [12], a success probability of $\approx 97\%$ can be realized. To achieve a detector efficiency of 90% for an optical photon, a modestly strong coupling with a Purcell factor of $\Gamma/\gamma = 10$ would be required. A different choice of α can be advantageous in different contexts, in particular for the Bell state analyzer discussed below.

V. BELL STATE ANALYZER

The photo detection schemes discussed above may be used in a variety of contexts where the measurement of more involved properties of light is required. A particularly important application is the design of an optical Bell state analyzer (BSA), which distinguishes the four Bell states

$$\begin{aligned} |\phi^\pm\rangle &= \frac{1}{2}\int \mathrm{d}k\mathrm{d}p\, f_1(k)f_1(p)\left(\hat{a}_{1k}^\dagger\hat{a}_{3p}^\dagger \pm \hat{a}_{2k}^\dagger\hat{a}_{4p}^\dagger\right)|0\rangle \\ |\psi^\pm\rangle &= \frac{1}{2}\int \mathrm{d}k\mathrm{d}p\, f_1(k)f_1(p)\left(\hat{a}_{1k}^\dagger\hat{a}_{4p}^\dagger \pm \hat{a}_{2k}^\dagger\hat{a}_{3p}^\dagger\right)|0\rangle, \end{aligned} \qquad (13)$$

where the subscripts $1-4$ refer to four different photonic modes. In principle, a BSA can be achieved directly from the scheme for photonic quantum gates in cavity QED [7]. Such setups, however, often require rapid switching of the optical path and delay lines for photons, which is experimentally unfavorable. Here, we consider a modified version of ref. [7], which avoids these elements and integrate it into a BSA. This setup shall be efficient and error-proof even for an imperfect coupling, i.e $\gamma \neq 0$, so that it cannot give a wrong measurement result.

For resonant input photons, the QND photo detector introduced above is sufficient to realize a simple error-proof BSA using the setup shown in fig. 4 (b). We assume that the logical state of both control and target photon are encoded into two spatial modes. The control photon (modes $\hat{a}_{1,2}$) passes the setup well before the target photon (modes $\hat{a}_{3,4}$). As described in the previous section, classical control pulses are applied to the emitters before and after the passage of each photon. Thus both the control and the target photon switch the internal state of the respective emitter as described in eqn. (12). For the Bell states $|\phi^{\pm}\rangle$, both photons pass the same arm of the setup subsequently. The emitter coupled to this arm is transferred from state $|g\rangle$ to $|s\rangle$ and back to state $|g\rangle$ after interacting with the control and target photon, respectively. The other emitter always remains in the internal state $|g\rangle$. On the contrary, the two photons pass through different arms of the interferometer for the Bell states $|\psi^{\pm}\rangle$, so that both emitters are transferred to the state $|s\rangle$. A measurement of the internal state of the emitters thus allows to distinguish between the subspaces spanned by $|\phi^{\pm}\rangle$ (atomic state $|gg\rangle$) on the one hand and $|\psi^{\pm}\rangle$ (atomic state $|ss\rangle$) on the other hand. Whether it is the plus or the minus sign is revealed by the coincidence pattern of detectors placed after a beamsplitter mixing the modes 1 and 2 as well as 3 and 4. For the plus (minus) states the photons will be detected in the modes 1+3 or 2+4 (1+4 or 2+3).

Taking into account photon loss, the success probability of this BSA is given by $p_{\text{success}} = \eta^2|t_0|^2 = \eta^2(\gamma-\Gamma)^2/(\gamma+\Gamma)^2$, where η is the efficiency of the final photo detectors (assuming $\alpha = 1/1-t_0$, see below). With non-resonant input, the probability for a successful Bell measurement including any transmission losses is given by

$$p_{\text{success}} = \frac{\eta^2|t_0|^2}{|1-t_0|^4}\int \mathrm{d}k\mathrm{d}p\,|f_2(k,p)(1-t_k)(1-t_p)|^2 \quad (14)$$

regardless of which of the Bell states is incident. This result (with $\eta = 1$) is plotted in fig. 4 (c) as a function of the loss rate γ/Γ for Gaussian input pulses. One finds that a Purcell factor of $\Gamma/\gamma \approx 5.8$ is sufficient to exceed the $\eta^2 \times 50$ % limit of linear optics.

The present setup is, however, not strictly error-proof if the input photons are not completely resonant. While the measurement result $|ss\rangle$ leads to an unambiguous Bell state measurement, the result $|gg\rangle$ does not. It can be almost certainly attributed to the subspace spanned by

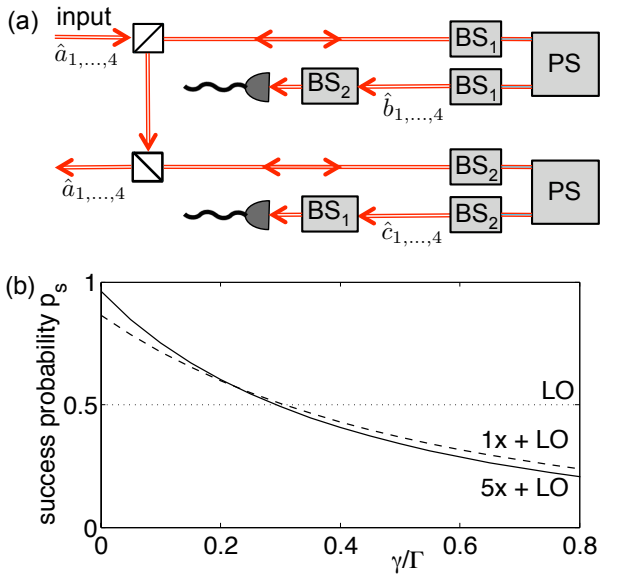

FIG. 5: (a) Setup of a BSA composed of two photon sorters (PS) and linear beam splitter arrays (BS_1 and BS_2, see text). The crossed squares are Faraday rotators and polarizers separating incoming and reflected modes. Each of the arrows represents four modes carrying the Bell state. (b) Total success probability of an array of $n = 1$ (1x + LO) and $n = 5$ (5x+LO) error-proof BSAs, plus a linear optical BSA at the end of the array as a function of the ratio γ/Γ assuming a Gaussian pulse shape with frequency width $\sigma/\Gamma = 0.36$. The success probability of a linear optical BSA (LO) is plotted for comparison.

$|\phi^{\pm}\rangle$, but there is a small probability that it has been triggered by the states $|\psi^{\pm}\rangle$. This error can, however, be suppressed to a large extend by choosing a rotation angle of $\alpha = 1/(1-t_0)$. In this case the residual probability to obtain an erroneous measurement result for the input state $|\psi^{\pm}\rangle$ is given by

$$p_{\text{error}} = \frac{\eta^2}{|1-t_0|^4}\int \mathrm{d}k\mathrm{d}p\,|f_2(k,p)(t_0-t_k)(t_0-t_p)|^2. \quad (15)$$

For a Gaussian wavepacket, p_{error} vanishes as $\sigma^4/(\gamma+\Gamma)^4$ for $\sigma/(\gamma+\Gamma) \to 0$. It thus remains small also for a non-monochromatic input photon as shown in fig. 4 (d).

In order to realize a fully error-proof BSA, one needs another measurement stage, which unambiguously detects $|\phi^{\pm}\rangle$. In principle this can be realized by exchanging the modes $\hat{a}_3$ and $\hat{a}_4$ and then repeating the above scheme. This would, however, require rapid switching of the optical path between control and target photon.

VI. A PASSIVE BELL STATE ANALYZER

The detection scheme described above realizes a perfect Bell state measurement in the ideal case, but requires a three-level system and an active control of the emitter.

As we will now show, a fully passive, error-proof BSA may in fact be constructed using the photon sorters introduced above. The setup to perform these operations is summarized in fig. 5 (a). Assume that the four optical modes containing the Bell state in eq. (13) are incident on a beam splitter array mixing the modes 1 and 4 as well as 2 and 3 (denoted by BS_1 in fig. 5). The states $|\psi^{\pm}\rangle$ are thereby mapped onto $\sim (\hat{a}_1^{\dagger 2} - \hat{a}_4^{\dagger 2} \pm \hat{a}_2^{\dagger 2} \mp \hat{a}_3^{\dagger 2})|0\rangle$, suppressing the pulse shape for simplicity. The two photons are always located in the same mode for the states $|\psi^{\pm}\rangle$, whereas they are always located in two different modes for the states $|\phi^{\pm}\rangle$. If each of the modes is now incident on the photon sorter introduced above, the states $|\psi^{\pm}\rangle$ are separated to the modes $\hat{b}_{1,\dots,4}$ with a significant probability. It is then possible to distinguish between $|\psi^{+}\rangle$ and $|\psi^{-}\rangle$ with linear optics and conventional photodetectors only, giving rise to an unambigious Bell state measurement. If no photon is detected we can simply go on with the two photons in the modes $\hat{a}_{1,\dots,4}$. In order to detect also the Bell states $|\phi^{\pm}\rangle$, one undoes the effect of the first beam splitter array BS_1 and then mixes the modes 1 and 3 as well as 2 and 4 instead (denoted by BS_2 in fig. 5). Now it's the states $|\phi^{\pm}\rangle$, for which the two photons are located in the same mode, these are thus separated to the modes $\hat{c}_{1,\dots,4}$ by the photon sorter and subsequently detected. The photons are either measured in the two detector arrays projecting unambiguously onto one of the Bell states or leave the BSA in the modes $\hat{a}_{1,\dots,4}$. In the latter case another measurement can be attempted.

The proposed BSA works probabilistically – with a non-vanishing probability the photons are not detected but just transmitted through the complete setup. The success probability is given by the probability of two photons to be scattered to the modes $\hat{b}_{1,\dots,4}$ or $\hat{c}_{1,\dots,4}$, respectively, and thus given by the success probability of the photon sorter, which is given in eq. (9) and plotted in fig. 2 (b). If the detection fails and the photons are transmitted, one can just repeat all operations. However, in actual experiments photon losses are inevitable and the coupling of the emitter to the one-dimensional waveguide is not perfect. Photon loss only leads to an inconclusive measurement result and fig. 5 (b) shows the resulting success probability of an array of 1 (dashed line) and 5 (solid line) concatenated BSAs, as a function of the ratio γ/Γ. After passing this array, we assume that the remaining modes are detected with a linear optical BSA. As shown in the figure already a modest Purcell factor of $\Gamma/\gamma \approx 3.3$ is sufficient to exceed the 50 % limit of linear optics.

VII. CONCLUSION

We have shown that the coupling of single emitters to one-dimensional waveguides opens up new possibilities for number resolving, non-demolition photo detection. We have explicitly shown how to construct photon sorters and QND detectors, and that these systems can be used for efficient Bell state analysis. Most importantly the devices are error-proof in the sense that imperfect coupling only leads inconclusive and not wrong results. As a consequence the devices work with modest coupling efficiencies, which are well within reach of current experiments.

Acknowledgments

Financial support by the German Research Foundation (DFG grant WI 3415/1), the Danish National Research Foundation and the Villum Kann Rasmussen foundation is gratefully acknowledged. Work at Harvard was supported by NSF, CUA, DARPA and Packard Foundation.

[1] Nogues G. *et al.* Nature **400** (1999) 239.
[2] Schuster D. I. *et al.* Nature **445** (2007) 515.
[3] Guerlin C. *et al.* Nature **448** (2007) 889.
[4] Johnson B. R. *et al.* Nature Physics **6** (2010) 663.
[5] Chang D. E., Sørensen A. S., Demler E. A. Lukin M. D. Nature Physics **3** (2007) 807.
[6] Thompson R. J., Rempe G. Kimble H. J. Phys. Rev. Lett. **68** (1992) 1132.
[7] Duan L.-M. Kimble J. Phys. Rev. Lett. **92** (2004) 127902.
[8] Reithmaier J. P. *et al.* Nature **432** (2004) 197.
[9] Yoshie T. *et al.* Nature **432** (2004) 200.
[10] Dayan B. *et al.* Science **319** (2008) 1062.
[11] Vetsch E. *et al.* Phys. Rev. Lett. **104** (2010) 203603.
[12] Astafiev O. *et al.* Science **327** (2010) 840.
[13] Chang D. E., Sørensen A. S., Hemmer P. R. Lukin M. D. Phys. Rev. Lett. **97**2006053002.
[14] Akimov A. V. *et al.* Nature **450** (2007) 402.
[15] Huck A., Kumar S., Shakoor A. Andersen U. L. Phys. Rev. Lett. **106** (2011) 096801.
[16] Shen J.-T. Fan S. Opt. Lett. **30** (2005) 2001.
[17] Shen J.-T. Fan S. Phys. Rev. Lett. **98** (2007) 153003.
[18] Shen J.-T. Fan S. Phys. Rev. A **76** (2007) 062709.
[19] Witthaut D. Sørensen A. S. New J. Phys. **12** (2010) 043052.
[20] Hwang J. *et al.* Nature **460** (2009) 76.
[21] Stobinska M., Alber G. Leuchs G. Europhys. Lett. **86** (2009) 14007.
[22] Imamoglu A., Schmidt H., Woods C. Deutsch M. Phys. Rev. Lett. **79** (1997) 1467.
[23] Lukin M. D. Imamoglu A. Phys. Rev. Lett. **84** (2000) 1419.
[24] André A., Bajcsy M., Zibrov A. S. Lukin M. D. Phys. Rev. Lett. **94** (2005) 063902.
[25] Duan L.-M., Lukin M. D., Cirac J. I. Zoller P. Nature **414** (2001) 413.
[26] Knill E., Laflamme R. Milburn G. J. Nature **409** (2000) 46.

[27] Lütkenhaus N., Calsamiglia J. Suominen K.-A. Phys. Rev. A **59** (1999) 3295.
[28] Dalibard J., Castin Y. Mølmer K. Phys. Rev. Lett. **68** (1992) 580.
[29] Bonato C. *et al.* Phys. Rev. Lett. **104** (2010) 160503.